Measurements of Terahertz Electrical Conductivity of Intense Laser-Heated Dense Aluminum Plasmas

K. Y. Kim, B. Yellampalle, J. H. Glownia, A. J. Taylor, and G. Rodriguez

Materials Physics and Applications Division, Los Alamos National Laboratory, Los Alamos, New Mexico 87545, USA

(Received 26 October 2007; published 3 April 2008)

We report the electrical conductivity of laser-produced warm dense aluminum plasmas measured using single-shot ultrafast terahertz (THz) frequency spectroscopy. In contrast with experiments performed at optical frequencies, measurements based upon THz probe reflectivity directly determine a quasi-dc electrical conductivity, and therefore the analysis does not require a free-electron Drude model based extrapolation to recover the near zero frequency conductivity. In fact, our experimental results indicate that the Drude model breaks down for warm (>0.6 eV), moderate-dense (<1.6 g/cm^3) aluminum at THz frequencies. A calculation of THz reflectivity over a non-Fresnel boundary in dense plasmas is also presented.

DOI: 10.1103/PhysRevLett.100.135002 PACS numbers: 52.25.Fi, 52.38.−r, 52.50.Jm

Upon heating, metals typically exhibit decreasing electrical conductivity due to enhanced electron-phonon scattering. However, if heated far beyond melting, it places the metal into a low-density hot plasma state where the conductivity then increases with temperature due to its lowered Coulomb collision rate between the electrons and ions. In between these two extremes, where the conductivity makes a turning point, a state of warm (0.1–10 eV) and dense (0.1–10 times the solid density) matter exists, which can be created in intense laser-produced laboratory plasmas, and is also thought to exist in a variety of extreme natural environments including brown dwarfs and the interiors of giant gaseous planets like Jupiter. In this so-called warm dense matter (WDM) regime, the ion-ion interaction is strongly correlated and the electrons are degenerate [1]. Lying between a solid state and an ideal plasma state, WDM is considered too dense to be depicted by the classical plasma theory and too hot to be described by solid-state physics. Because of this complexity, it is generally difficult to determine the equation of state for WDM. Furthermore, detailed experimental reports are sparse. Aside from challenges related to creating WDM, it is also difficult to precisely characterize WDM where techniques to measure the transport properties are often applied. This paucity of experimental information limits the development of advanced theoretical models, such as density functional theory and quantum molecular dynamics [2], which are presently considered the most successful at describing WDM.

As stated above, an established experimental approach to characterizing WDM is through measurements of its transport properties such as electrical and thermal conductivities. Previous studies of electrical conductivities have been performed by employing electrically exploding wires [3–5] or foils [6] and measuring the current and voltage change across the formed WDM plasma, or by using optical probe reflectivity measurements from laser-heated solids [7–12]. In the latter case, the measurements provide the ac electrical conductivity because the probe is at optical frequencies. However, since knowledge of the dc component is actually desired, the dc electrical conductivity is obtained by applying a free-electron Drude model, in which the ac electrical conductivity is given as $\sigma(\omega) = \sigma_0/(1 - i\omega\tau)$, with σ_0 as the dc conductivity, ω the electromagnetic pulse angular frequency, and τ the electron relaxation time. To further complicate matters, recent theoretical models predict non-Drude behavior for WDM at low frequencies even for relatively simple metals such as aluminum [13–15], making the general applicability of a Drude model based analysis questionable.

To address this issue, here we apply ultrafast terahertz (THz) spectroscopic techniques to directly measure the quasi-dc electrical conductivity, which, in principle, does not require any extrapolation based upon a Drude model. This is true because in the Drude limit for dense materials, the real part of THz conductivity is expressed as $\sigma_{r,\mathrm{THz}} = \sigma_0(1 + \omega_{\mathrm{THz}}^2\tau^2)^{-1} \approx \sigma_0$, and the value of $\omega_{\mathrm{THz}}\tau$ is only 0.008 at 1 THz for room temperature aluminum. In addition, by using a broadband THz electromagnetic probe pulse approach, we are able, for the first time, to critically evaluate the validity of a Drude model analysis for WDM at low (THz) frequencies.

Our experimental setup is shown in Fig. 1. An amplified Ti:sapphire laser system capable of delivering 815 nm, 50 fs, 30 mJ pulses at a 10 Hz repetition rate is used. The laser pulse width is stretched to $\sim$140 fs (FWHM) to avoid nonlinear effects in the optics and air in the beam path. Most of the pulse energy is used to heat an aluminum ($>99.0\%$) slab target focused to a spot size of $\sim$1 mm (FWHM) yielding peak intensities of $\sim 10^{13}$ W/cm^2. Here, the relatively large pump spot size ($\sim$millimeter) is necessary to overfill the diffraction limited THz focal spot. We note that the native oxide surface on the target plays little or no role because its thickness ($\sim$2 nm) [7] is more

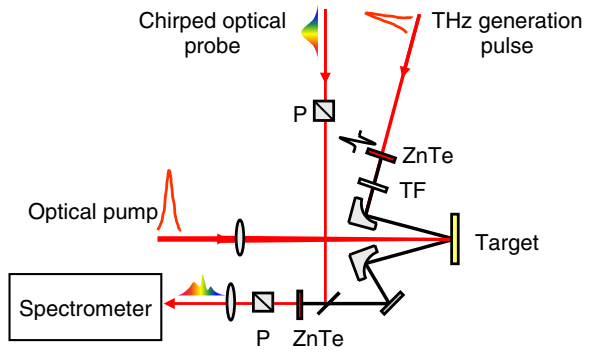

FIG. 1 (color online). Schematic of experimental layout, showing optical pump, chirped probe, THz pulses, THz generation, and detection ZnTe crystals, Teflon filter (TF), polarizers (P), and spectrometer.

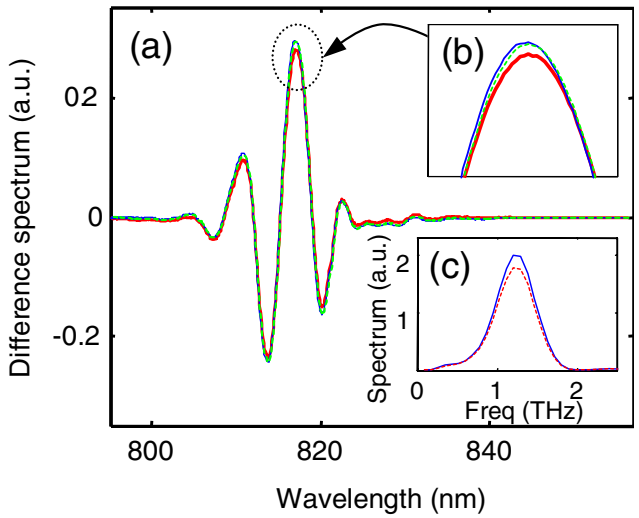

FIG. 2 (color online). (a) Background-subtracted optical spectra with optical pump on (blue line), off (thick red line), and THz alone after the pump shot (dashed green line). (b) Close-up for the difference spectra. (c) THz spectra with pump off (solid blue line) and on (dashed red line).

than an order of magnitude smaller than the THz skin depth. A portion of laser energy is directed to a 1-mm thick ZnTe [110] crystal generating THz pulses via optical rectification. A 3-mm thick Teflon window is placed after this crystal to block unwanted optical pulse leakage into the detection arm, while transmitting the generated THz pulses. The THz probe pulse, tightly focused by an off axis parabolic mirror, is incident on the sample at angle of $\theta \approx 20°$ with p polarization. To match the pump and probe spot sizes on the sample, an anodized iris diaphragm with a $\sim$2 mm aperture diameter is placed in front of the sample. Because of the relatively small aperture size compared to the THz wavelength, only high frequency components ($\geq$0.3 THz) of THz pulses probe the laser-heated area. The reflected THz probe is collected and focused by another off axis parabolic mirror into a second 1-mm thick ZnTe crystal for its detection. An additional optical pulse, split from the main laser and chirped to $\sim$2.6 ps (FWHM) by a pair of gratings, is used to measure the THz probe waveform in a single shot with a spectrograph detector based electro-optic sampling technique [16]. Figure 2 shows typical THz reflectivity experimental results at a probe delay of $\sim$60 ps with 12 mJ of pump energy. Figure 2(a) shows three optical spectra—with pump off and THz on (blue line), both pump and THz on (thick red line), and THz alone (dashed green line), all normalized by subtracting the pump and THz off background spectrum. With direct frequency-to-time mapping of the chirped optical pulse [16], these spectra represent THz waveforms of the reflected probe. A small but noticeable THz reflectivity change with laser heating is evident in the blowup inset [Fig. 2(b)]. Because of the small ($<$5%) THz reflectivity change and limited sample size, averaging a series of 20 pump shots at the same spot location is required. To check possible effects due to sample ablation, a pump-free THz reflectivity measurement is made following a series of pump shots (dashed green line) and then compared with the prepump-shot case (blue line). Small differences, as shown in Fig. 2(b), indicate the THz probe reflectivity is nearly unaffected by the accumulated ablation-induced, microstructured damage on the target surface, consistent with the long wavelength of the probe pulse. The Fourier-transformed THz spectra with pump off (solid blue line) and on (dashed red line) are shown in Fig. 2(c), indicating a reduced THz reflectivity (or conductivity) upon laser heating of the sample.

Figure 3 shows THz reflectivity from laser-heated aluminum as a function of THz frequencies for various pump energies at a pump-probe delay of $\sim$10 ps. For low pump energies, the reflectivity follows a Drude-like response, where the reflectivity increases with decreasing THz fre-

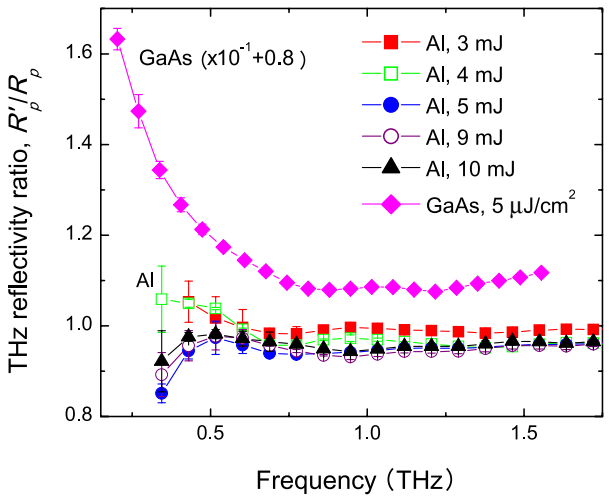

FIG. 3 (color online). THz reflectivity from laser-heated aluminum and photoexcited GaAs as a function of frequency for various optical-pump energies.

quencies. In this regime, the dielectric function can be approximated as $\varepsilon(\omega) = \varepsilon_\infty - \omega_p^2/(\omega^2 + i\omega\nu) \approx i\omega_p^2/(\omega\nu)$ at THz frequencies ($\omega \ll \nu < \omega_p$), where ω_p is the plasma frequency and ν is the electron-ion collisional frequency. Here a simple Fresnel reflectivity expression at normal incidence is $R \approx 1 - 2\sqrt{2\omega\nu}/\omega_p$. As shown in Fig. 3, such a Drude-like reflectivity is clearly evident in a photoexcited GaAs which undergoes a semiconductor-to-conductor transition upon photoexcitation. By contrast, as the pump laser energy is increased, the THz reflectivity from laser-heated aluminum is found to decrease for frequencies <0.5 THz. Such a collapse of low frequency conductivity, which deviates from a Drude response, is predicted in recent simulations [13,15] and is interpreted as being due to the formation of a pseudogap at the Fermi energy for moderate-density (<1 g/cm^3) aluminum plasmas [13,15]. This leads to an optical conductivity enhancement between 4 and 6 eV and simultaneous suppression of the near dc conductivity.

Time-resolved THz reflectivity at a peak intensity of $\sim 10^{13}$ W/cm^2 is also measured and plotted in Fig. 4(a) where the THz reflectivity (or conductivity) gradually decreases with time. One interesting feature to note is the large conductivity swing near $t = 0$. This is attributed to self-generation of THz from the laser-heated area by the optical pump, which interferes with the THz probe pulse, and is confirmed by detecting the emitted THz radiation in the absence of THz probe. We speculate that a subpicosecond current surge, possibly arising during the interaction, is responsible for the THz generation, and the mechanism for this is currently under investigation.

From the THz reflectivity, the corresponding dielectric function $\varepsilon(\omega)$ for laser-heated aluminum is obtained via Fresnel's equation $r_p = [-\varepsilon(\omega)\cos\theta + \sqrt{\varepsilon(\omega) - \sin^2\theta}]/[\varepsilon(\omega)\cos\theta + \sqrt{\varepsilon(\omega) - \sin^2\theta}]$ for p polarization at an incidence angle of θ. From the measured reflectivity ratio $\hat{r}_p \equiv r'_p/r_p$, where r'_p and r_p denote the reflection amplitude with and without laser heating, respectively, and using the known room temperature value of $\varepsilon = -3.37 \times 10^4 + i5.45 \times 10^5$ at 1.2 THz [17], one can obtain the laser-heated dielectric function ε', as well as the electrical conductivity, $\sigma' = \sigma'_r + i\sigma'_i$, where $\sigma'_r = \omega\,\mathrm{Im}[\varepsilon']/(4\pi)$ and $\sigma'_i = \omega[1 - \mathrm{Re}[\varepsilon']]/(4\pi)$. The line with triangles in Fig. 4(a) shows σ_r at 1.2 THz. Here, the use of Fresnel's equation is valid only for a sharp plasma boundary ($L \ll \delta_{\mathrm{THz}}$), where L is the scale length of the plasma density gradient and δ_{THz} is the skin depth at the THz frequency (for $L \geq \delta_{\mathrm{THz}}$, see below). Figure 4(b) shows the measured THz reflectivity (line with squares) at 1.2 THz and the corresponding conductivity (line with triangles) for increasing laser intensity at a ~10 ps pump-probe delay. Initially, the conductivity decreases with increasing laser intensity, but it soon saturates over an extended range beyond $\sim 5 \times 10^{12}$ W/cm^2. This onset of conductivity (or resistivity) saturation, which typically occurs when the

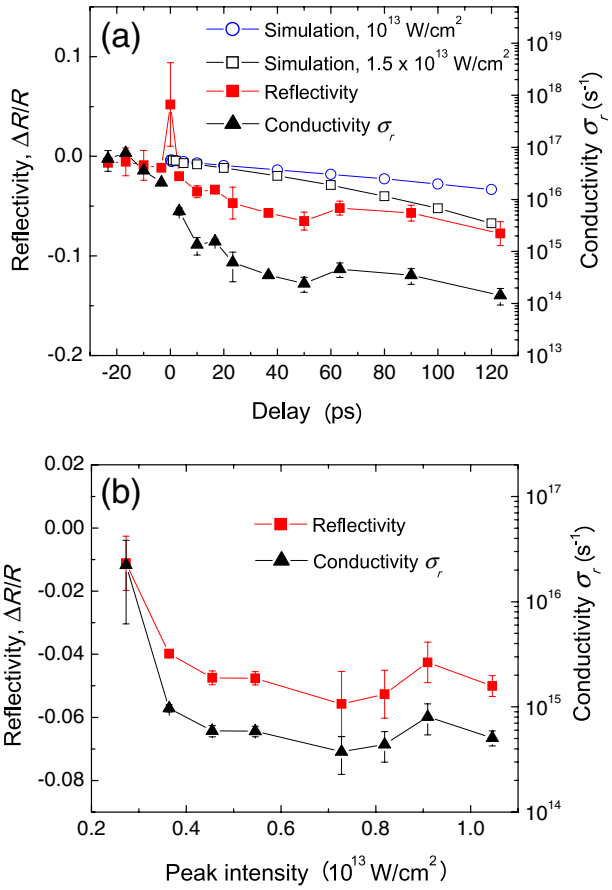

FIG. 4 (color online). (a) Time-varying THz probe reflectivity (line with squares) and the corresponding real part of electrical conductivity σ_r (line with triangles) at 1.2 THz, along with computed THz reflectivity using the dielectric function gradient obtained from the hydrocode. (b) Time-varying THz reflectivity and σ_r with increasing pump laser intensity.

electron mean free path becomes comparable to the interatomic separation regardless of its disorder, was previously reported using optical reflectivity measurements [7], but at an order of magnitude higher intensity (10^{14} W/cm^2) than reported here. This discrepancy, we believe, arises due to the lower aluminum mass density (1.6–2.7 g/cm^3) in our case, resulting from the hydrodynamic expansion over ~10 ps (see Fig. 5). This not only decreases the conductivity but also saturates the mean free path at much lower laser intensities.

To determine how deeply the THz probe propagates into the density gradient, we have numerically solved the time-independent Helmholtz equation for the magnetic field B [7], $d^2B/dx^2 - \varepsilon^{-1}(d\varepsilon/dx)(dB/dx) + k^2(\varepsilon - \sin^2\theta)B = 0$, via a matrix transfer method. In this determination, the dielectric function is given as $\varepsilon(x, \omega) \approx 1 + i4\pi\sigma_0(x)/\omega$ [18], where x is the coordinate in the density gradient direction, and $\sigma_0(x) = (N_e e^2 \tau/m)A^\alpha(\mu/kT)$ is the dc electrical conductivity based on the Lee and More model [19], where A^α is a function of μ/kT and μ is the chemical

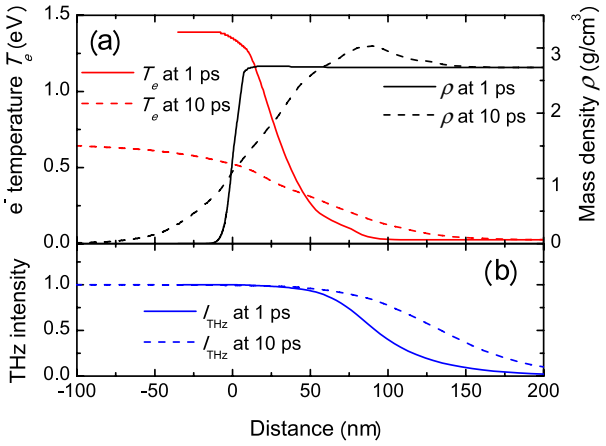

FIG. 5 (color online). (a) Electron temperatures T_e and mass densities ρ profiles at 1 and 10 ps pump-probe delays obtained from HYADES hydrocode simulations. (b) Computed THz probe penetration into the density gradient.

energy. Here, $\sigma_0(x)$ is computed using one-dimensional hydrodynamic simulations (HYADES) [20] incorporating a Helmholtz wave solver for calculation of the interaction of the short pulse electric field at the surface. Figure 4(a) shows the result of this simulation (lines with open circles and squares), and a discrepancy between the simulation and experiment is apparent at early delays (<20 ps), indicating the measured conductivity is at least an order of magnitude lower than the conductivity computed using the Lee and More model. Figure 5 shows HYADES simulation results for electron temperature (T_e) and mass density (ρ) at $t = 1$ ps and 10 ps, along with THz probe intensity profiles obtained from solution to the Helmholtz equation. The THz skin depth δ_{THz}, which is ~74 nm at 1.2 THz for room temperature aluminum, increases with laser heating and the density gradient scale L. The calculation shows deep penetration (~200 nm at 10 ps) of the THz field into the gradient. The average T_e and ρ over the density gradient, weighted by the THz intensity, are $T_e \sim 0.9$ eV, $\rho \sim 2.6$ g/cm^3 at 1 ps, and $T_e \sim 0.6$ eV, $\rho \sim 1.6$ g/cm^3 at 10 ps. From Fig. 4(a), the conductivity $\sigma_r(1.2\ \mathrm{THz}) \approx \sigma_0 \sim 10^{16}\ \mathrm{s}^{-1}$ and $\sim 10^{15}\ \mathrm{s}^{-1}$ at 1 and 10 ps, respectively, which are in a good agreement with previous experiments [5,9].

In conclusion, we report electrical conductivity measurements of laser-heated aluminum using ultrafast optical-pump, THz probe reflection spectroscopy. Unlike ac conductivity measurements performed using an optical probe, our THz measurement provides direct quasi-dc electrical conductivities without reliance upon a free-electron Drude model. In fact, for warm (>0.6 eV) moderate-dense (<1.6 g/cm^3) aluminum, the analysis indicates a breakdown of the Drude model at relatively low THz frequencies. These results suggest that THz spectroscopy can be a powerful quantitative characterization tool applicable to a variety of WDM creation methods, including x-ray heating, thin foil explosion [11,12], and ion beam heating to create a single-state WDM necessary for equation of state characterization. In particular, since we determine a relatively long skin depth at THz frequencies, a convenient transmission geometry is readily feasible with thin (<100 nm) samples.

This work was supported through the Los Alamos National Laboratory Directed Research and Development Program.

[1] S. Ichimaru, Rev. Mod. Phys. **54**, 1017 (1982).
[2] R. Car and M. Parrinello, Phys. Rev. Lett. **55**, 2471 (1985).
[3] A. W. DeSilva and J. D. Katsouros, Phys. Rev. E **57**, 5945 (1998).
[4] I. Krisch and H.-J. Kunze, Phys. Rev. E **58**, 6557 (1998).
[5] J. F. Benage, W. R. Shanahan, and M. S. Murillo, Phys. Rev. Lett. **83**, 2953 (1999).
[6] P. Renaudin, C. Blancard, G. Faussurier, and P. Noiret, Phys. Rev. Lett. **88**, 215001 (2002).
[7] H. M. Milchberg, R. R. Freeman, S. C. Davey, and R. M. More, Phys. Rev. Lett. **61**, 2364 (1988).
[8] A. Ng *et al.*, Phys. Rev. Lett. **72**, 3351 (1994).
[9] A. N. Mostovych and Y. Chan, Phys. Rev. Lett. **79**, 5094 (1997).
[10] H. Yoneda, H. Morikami, K. Ueda, and R. M. More, Phys. Rev. Lett. **91**, 075004 (2003).
[11] K. Widmann *et al.*, Phys. Rev. Lett. **92**, 125002 (2004).
[12] Y. Ping *et al.*, Phys. Rev. Lett. **96**, 255003 (2006).
[13] M. P. Desjarlais, J. D. Kress, and L. A. Collins, Phys. Rev. E **66**, 025401(R) (2002).
[14] S. Mazevet, M. P. Desjarlais, L. A. Collins, J. D. Kress, and N. H. Magee, Phys. Rev. E **71**, 016409 (2005).
[15] G. Faussurier, C. Blancard, P. Renaudin, and P. L. Silvestrelli, Phys. Rev. B **73**, 075106 (2006).
[16] K. Y. Kim *et al.*, Appl. Phys. Lett. **88**, 041123 (2006).
[17] M. A. Ordal *et al.*, Appl. Opt. **22**, 1099 (1983).
[18] $\varepsilon(x, \omega) = 1 + i4\pi\sigma(x, \omega)/\omega$ with a Drude model based $\sigma(x, \omega) = \sigma_0(x)/[1 - i\omega\tau(x)]$ gives almost the same results.
[19] Y. T. Lee and R. M. More, Phys. Fluids **27**, 1273 (1984).
[20] J. Larson, Cascade Applied Science Inc., Boulder, Colorado.